Properties of waves reflected off the Earth's core boundaries

Dmitry Bobrov[1], Petr Kaazik[2], Ivan Kitov[2], Dmitry Krasnoshchekov[2] and Vladimir Ovtchinnikov[2]

1- CTBTO, Vienna, Austria, 2 – Institute of Dynamics of Geospheres of Russian Academy of Sciences, Moscow, Russia

I. OBSERVATIONS

We report on significant extention of database of joint PcP and PKiKP measurements (Fig. 1) on records of underground nuclear explosions and earthquakes throughout the world. An important part of waveforms has come from seismic arrays of the International Monitoring System of the Comprehensive Nuclear-Test-Ban Treaty Organization (CTBTO). Events were selected with the help of IDC REB, which yields 370 PKiKP measurements after deep events recorded by 65 stations (Fig. 2).

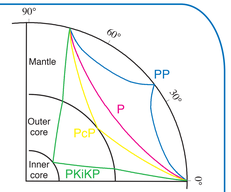

Fig. 1. Geometry of the ray paths of P, PP, PcP and PKiKP.

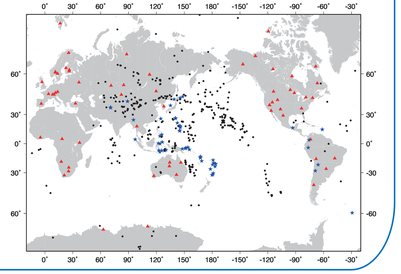

Fig. 2. Map with locations of IMS seismic stations and arrays (red triangles), seismic sources (blue stars) and projections of PKiKP reflection points on daylight surface (black dots).

II. PROCESSING

The processing was aimed at measuring amplitudes, periods and spectral content of PcP and PKiKP waveforms. Both waves at narrow angle reflections are essentially weak arrivals often obscured by seismic coda. To detect the sought waveforms and increase signal-to-noise ratio, we used frequency filtering and beamforming of array data. In particular, there were used linear and phase weighted summation of traces (Fig. 3). Cross-correlation techniques were used for measuring PKiKP-PcP differential travel times (Fig. 4).

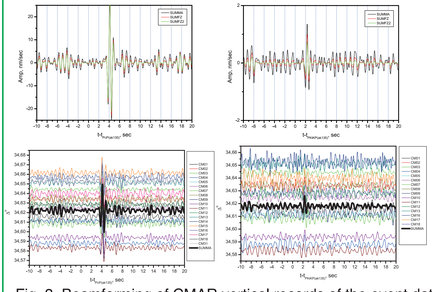

Fig. 3. Beamforming of CMAR vertical records of the event dated May 1, 2003 (7.25°S;122°E; 577.8 km; 04:02:05.44; mb=5.3). Bottom: bandpass (1-2 Hz, 5 poles) filtered records and linear beam for PcP (left) and PKiKP (right). Top: beams for linear (black), phase weighted (red) and phase weighted with squared coefficients (green) summations.

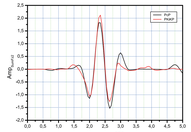

Fig. 4. Cross-correlation of PcP and PKiKP waveforms after the event from Fig. 3 also recorded at Chiang Mai (CMAR) in Thailand.

Reliability of detections of PcP and PKiKP waveforms is confirmed by ***f-k*** analysis. Fig. 5 shows and example for the array records of the Chinese explosion dated August 15, 1995 and registered by the Australian array ASAR.

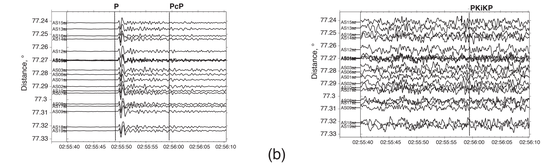

Fig. 5. Raw data (a) and results of ***f-k*** analysis (b) performed for ASAR array records of a Chinese explosion. Slowness diagrams given from left to right in the (b)-pane are calculated for time periods corresponding to the arrivals of P, PcP and PKiKP waves respectively.

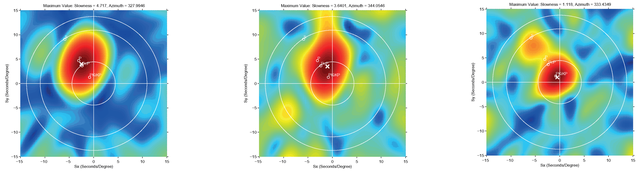

Additionally, seismic coda decay curves were calculated over the array data. An example for the FINES array is given in Fig. 6.

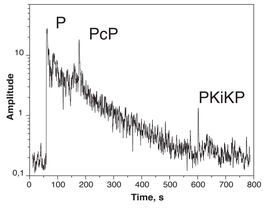

Fig. 6. The seismic coda decay curve is essentially maxima of slowness diagrams calculated over array data in a sliding window and plotted versus time. 1.5-second sliding window and square root beam amplitudes were used for the above given curve. The growth in beam amplitudes in the form of an archafter the arrival of PKiKP is PKiKP coda.

III. RESULTS

Amplitudes. Measured PKiKP amplitudes are given in Fig. 7. We observe significant discrepancy between predictions with respect to the model with sharp ICB and experimental data (especially in the transparent zone). A better agreement is reached if shear waves' velocity is set to 2 km/s in the inner core. In the same time this value differs from the value of 3.64 km/s obtained from the normal mode data.

Spectral content. Fig. 8 shows spectral ratio for different phases, that evidences a higher frequency content of PKiKP wave comparing to PcP. Measurements of PKiKP and PcP periods are given in the table below and show discrepancy between PKiKP and PcP periods with probability error P below 0.07. The statistics of measured PKiKP periods yields a multi-mode function (Fig. 9) with distinct peaks at 0.5-0.7 s, 0.7-0.9 s and 1.1-1.2 s. The amplitude of peaks decreases with period growth. Spatial distribution of PKiKP measured periods was built by Criging method (Fig. 10). It shows longer periods of 1.1 s are tend to be observed closer to polar regions, while observations around 0.7 s - to the equatorial ones.

Coda decay curves. We observe two types of curves: (i) with sharp onset and smooth decay and (ii) smoothly growing coda with no clear parent phase.

Interpretation. Three types of the inner-outer core transition are viable (Fig. 11). Sharp boundary like in PREM, but with heterogeneities in the uppermost inner core. A transition with thin layer in the bottom of the outer core, and a transition with a layer in the top of the inner core. Fig. 7 shows theoretical PKiKP amplitude predictions for the latter two models, that are also the limiting alternatives describing the experimental measurements. Complex distribution of the observed PKiKP periods can be due to inner core growth or rotation, that influence the mosaic patches in essentially different way in the polar and equatorial regions.

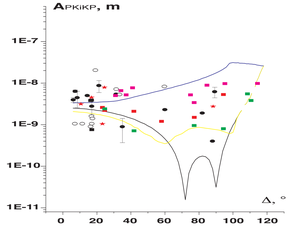

Fig. 7. Measured PKiKP amplitudes reduced to magnitude 5.9 and theoretical predictions for PKiKP amplitudes with respect to PREM (black curve) and PREM modifications with liquid thin transition layer (blue curve) and solid layer (yellow curve). Magenta rectangles - PKiKP measured amplitudes after the Pamir earthquake, red rectangles and stars - Chinese explosion dated 08/06/96, green rectangles - dated 17/08/95, and black rectangles - dated 15/05/95. Hollow and filled black ovals are from *Nature*, **435**, 483 (2005) by *Krasnoshchekov et al.*

!

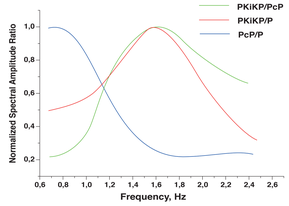

Fig. 8. Normalized spectral amplitude ratios calculated for seismic phases P, PcP and PKiKP detected on the vertical component of ZRN short-period record of station ZRN that registered a Chinese explosion.

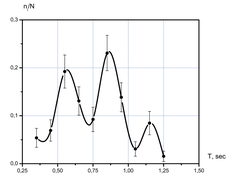

Fig. 9. The multi-mode function of distribution of measured PKiKP periods. To prevent possible influence of magnitude, only events with body wave magnitude between 5.7 and 5.9 were selected. Averaging of the whole dataset does not change the pattern.

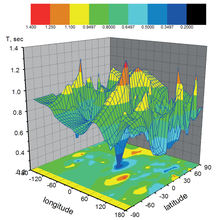

Fig. 10. Measured PKiKP periods plotted versus geographic coordinates of PKiKP reflection point on the surface of the inner core.

Phase	PcP			PKiKP			t-statistics	P
Date	T, s	σ, s	n	T, s	σ, s	n		
07.10.94	0.67	0.083	13	0.54	0.133	14	3.0996	0.005
15.05.95	0.66	0.089	5	0.52	0.079	10	2.9914	0.010
17.08.95	0.68	0.177	16	0.57	0.125	12	1.8723	0.073
08.06.96	0.69	0.13	13	0.53	0.15	9	2.7354	0.012

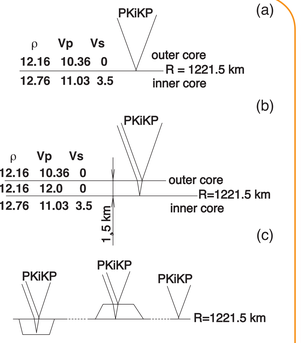

Fig. 11. Reflections from the inner core and appropriate physical parameters with viable structures of the inner core boundary: (a) - PREM, (b) - PREM modification with a global liquid transition layer in the bottom of the outer core, (c) - mosaic structure of the inner core's surface, where patches of sharp transition are interspersed with patches featuring thin transition layers either in the bottom of the outer core or in the outermost inner core.

IV. CONCLUSIONS

Being a powerful monitoring means of CTBTO, IMS array data provide good opportunity to study deep Earth structures. Long registration history and geographically diverse locations of IMS stations increase their value in terms of geophysical investigation. Here we analyze the joined dataset to study inner core boundary. From experimental data we infer the inner core boundary is essentially a region with its fine structure whose basic elements are thin plates located either in the top of the solid core or in the bottom of the liquid core. Such a structure is capable of accounting for changes in PKiKP amplitudes with growth of epicentral distance, relatively high PKiKP frequency content and coda formation in the form of separate pulses. The scattered PKiKP waves observed in the form of an arch after the parent phase indicate heterogeneities of the upper inner core. The derived structural peculiarities of the inner-outer core transition contribute to uncertainty of the estimates of the density jump on the inner core boundary using PKiKP/PcP amplitude ratio.

V. ACKNOWLEDGEMENTS

A part of the processed data was supplied under the current vDEC Contract between PTS and IDG RAS for limited access to IMS data and IDC products regarding a project entitled "Improving travel time prediction for secondary P-waves using IMS array stations".